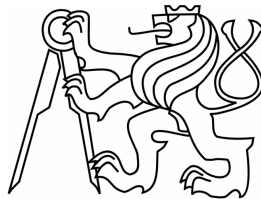


CZECH TECHNICAL UNIVERSITY IN
PRAGUE

FACULTY OF NUCLEAR SCIENCES AND PHYSICAL
ENGINEERING

Department of Physics



BACHELOR THESIS

**Electroproduction of Kaons on
Nucleons**

Dalibor Skoupil

2010

Supervisor: RNDr. Petr Bydžovský, Csc.

Prohlášení

Prohlašuji, že jsem svou bakalářskou práci vypracoval samostatně a použil jsem pouze podklady uvedené v příloženém seznamu.

Nemám závažný důvod proti užití tohoto školního díla ve smyslu §60 Zákona č.121/2000 Sb., o právu autorském, o právech souvisejících s právem autorským a o změně některých zákonů (autorský zákon).

V Praze dne _____

Dalibor Skoupil

Acknowledgement

I would like to thank my supervisor RNDr. Petr Bydžovský, Csc. for his willingness, for his continuous support during writing of this thesis, for the amount of information he gave me about this topic and for many useful hints, which helped me.

In addition, I would like to thank to all the people in my surroundings for their support and assistance.

Název práce: **Elektroprodukce kaonu na nukleonech**

Katedra: Katedra fyziky

Autor: Dalibor Skoupil

Obor: Jaderné inženýrství

Druh práce: Bakalářská práce

Vedoucí práce: RNDr. Petr Bydžovský, Csc.

Abstrakt: Produkce pseudoskalárních mezonů (pion, eta, kaon) na nukleonech indukovaná elektrony při nízkých energiích je proces vhodný pro zkoumání vlastností a dynamiky baryonů a jejich rezonancí. Zajímavým procesem je produkce kaonu, při které vzniká pár podivných kvarků. Pochopení a dobrý popis procesu produkce kaonu v asociaci s hyperonem jsou důležité pro výpočty účinných průřezů elektroprodukce hyperjader. Obsahem bakalářské práce je seznámení se s problematikou isobarického modelu pro foto a elektroprodukcí kaonu na nukleonech a získání orientace v dané oblasti.

Klíčová slova: elektroprodukce, fotoprodukce, kaon, produkce podivnosti, nukleonové rezonance

Thesis title: **Electroproduction of Kaons on Nucleons**

Department: Department of Physics

Author: Dalibor Skoupil

Branch of study: Nuclear Engineering

Kind of thesis: Bachelor's Degree Project

Supervisor: RNDr. Petr Bydžovský, Csc.

Abstract: The production of pseudoscalar mesons (π , η , K) on nucleons induced by low-energy electrons is suitable process for investigating the properties and dynamics of baryons and their resonances. Because of the creation of the pair of strange quarks, the interesting process is the kaon production. An understanding and a good approach of the kaon production process with association of hyperon is very important for calculations of cross sections of hypernuclei electroproduction.

 The aim of this bachelor thesis is to get familiarised with the isobar model problematics for the photo- and electroproduction of kaons on nucleons and to get orientation in the given area.

Keywords: electroproduction, photoproduction, kaon, strangeness production, nucleonic resonances

Contents

1	Preface	1
2	Introduction to the Particle Production	3
2.1	Why do we study particle production reactions?	5
2.2	How to study particle production?	6
2.3	What are the advantages of (γ^*, K) ?	8
2.4	Historical Background	9
3	Approaches to the Description of Particle Production Processes	11
3.1	χ PT, Quark Model, Regge Formalism, Regge-Plus-Resonance Approach	12
3.2	Coupled-Channel Approach	14
4	Isobar Model	17
4.1	The Effective Lagrangian	19
4.2	An Illustrative Calculation	20
4.3	Properties of the Model	22
4.3.1	Resonances	22
4.3.2	Coupling Constants	22
4.3.3	Hadronic and Electromagnetic Form Factors	23
4.3.4	Amplitudes and Observables	24
5	Demonstrative Calculations and Graphs	26
6	Conclusion	30

A The Hadron Current	31
A.1 CGLN Amplitudes	32
B Feynman diagrams	34
B.1 The Rules for the Construction and Interpretation of Feynman Diagrams	35

Chapter 1

Preface

The aim of this work is to deal with the production of pseudoscalar mesons on nucleons induced by electrons at energy of few GeV. This process is suitable for investigating the properties of baryons and their resonances. The tool for studying this process are models based on the tree-level perturbation theory of the effective hadron Lagrangian. Free parameters in the Lagrangian are determined by the fitting on the experimental data.

It is believed, that the particle electromagnetic production will bring some deeper insight into the structure of hadrons. Therefore, it is an important and very promising field of study. Moreover, thanks to the particle production, one can study the resonance properties.

Although there are many ways to study the particle production, the most challenging process is the kaon photo- and electroproduction. Since the electromagnetic part of the process is well understood, the kaon production is relatively easy to describe.

In this thesis, the second chapter is related to a brief introduction. There are shown reasons why and how to study the particle production. The historical background is outlined there, too. After that in the third chapter, we introduce some approaches to the description of the particle production

processes. Among them, the isobar model, which is presented in the fourth chapter, is of particular interest.

After all, there are some demonstrative calculations and graphs, which shows the cross sections calculated using the Kaon-MAID model in comparison with the experimental values.

Chapter 2

Introduction to the Particle Production

In history, the strongest motivation for the scientific progress has always been the desire to find out how do things work and to see beyond the limits of our everyday experience of space and time. Everytime in the past, people were mesmerized with the universe with the amount of stars. In the cores of stars, there are observed phenomena, which on Earth only occur under artificial circumstances in the laboratories or in particle accelerators. No wonder, that this fascination with the universe led to growing interest in processes at ever smaller distance scales. It is believed, that research of this orientation is essential to understand the processes occurring in the universe.

A milestone in our understanding of the microscopic world has been the development of the Standard Model (SM). In this model, all elementary particles are sorted into two categories of bosons, the elementary particles with an integer spin, and fermions, the elementary particles with a half-integer spin. The fermions are leptons (e.g. electron, muon, tau) and quarks, which form the hadrons (e.g. proton, neutron). Moreover, it seems that all processes

occurring in the nature can be described on the basis of only four fundamental forces: the strong, weak, electromagnetic, which are understood to be mediated by the exchange of gauge bosons and are treated uniquely by the SM, and the gravity (which is the weakest force).

The three standard-model forces are very well understood. For each of them, a field-theoretical framework is available which describes how the bosons mediating the force couple to the elementary fermions. However, the knowledge of the behavior of the fundamental constituents of matter does not guarantee an understanding of larger-scale processes (e.g. the low-energy hadron-hadron scattering). In this respect the strong interaction, described by the theory of quantum chromodynamics (QCD), is the most challenging. The structure of QCD causes the behaviour of the strong coupling constant α_s , which measures the strength of the force that holds quarks and gluons together to form the proton, the neutron and other particles, is different than the behaviour of the electromagnetic coupling constant. At large distances between interacting particles (e.g. a small energy or momentum transfer), the strong coupling constant does not decrease, as the electromagnetic constant, but increases, which causes the perturbation scheme of calculations cannot work well.

One very interesting effect of this behavior is called confinement. The confinement causes that quarks cannot be observed as free objects, but only in bound states - hadrons. The constituent quarks in a hadron cannot be separated from the bound state because of the steeply rising interaction with gluons and sea quarks (this is the reason why quarks can never be studied or observed in any more direct way than at a hadron level).

The main objective of the study in hadronic physics is to gain insight into the transition between quark-gluon and hadronic degrees of freedom. Over the years, considerable effort has been invested into improving the

existing picture of the nucleon spectrum. In this case, the knowledge of the nucleon excitations (resonances) is expected to provide essential information concerning the behavior of quarks at hadronic scales.

2.1 Why do we study particle production reactions?

There are two good reasons why to study the particle production. Analysing the processes, we can gain a deeper insight into the hadron structure as well as investigate the resonance properties.

In order to get better insight into the structure of hadrons (in this case nucleons) it is important to fully understand its excited states. It is the spectrum of nucleonic excitations which reflects its internal structure and must contain some kind of sign of the constituents at a lower level. Information about the nucleon resonances can be collected from the amount of experiments performed at world laboratories (we can mention e.g. CEBAF, ELSA, MAMI, SPring-8 etc., where the photo- or electroproduction processes are realised) [4].

In the last few decades, a plenty of information concerning the nucleon spectrum has been gathered. It is the pion induced and pion production reaction, we can owe it for. However, it has been realized, that pionic reactions might be overly restrictive with regard to the specific type of intermediate resonant state, which can be excited [4]. This assumption is supported by quark model calculations predicting far more excited states than have been registered in pion production experiments. This observation is known as the “missing resonance” phenomenon in medium particle physics.

There is a question, whether we can observe those “missing resonances” in decay channels which do not involve a pion or whether there is something seriously wrong with the present quark model as the essence of our perceiving

of the structure of hadrons.

Recently, the photo- and electroproduction reactions that involve strangeness in the final state have internationally received a lot of attention. It is believed, that the presence of a strange quark pair $s\bar{s}$ in the reaction dynamics in addition to the *up* and *down* quarks can shed a new light on the understanding of the spectrum and dynamics of hadrons. Therewithal, the quark models predict decay of some of the missing resonances into the strange channels [4,9].

All this mentioned above makes the strangeness production a very promising field of study.

2.2 How to study particle production?

There are several ways how to study the particle production, and therefore the information can be gathered from a variety of experiments. Most of the available information about the nucleon resonances was gathered in experiments involving pion-nucleon final states. The production of strange particles in the final state can also be achieved in the reactions with hadron beams, e.g. $n(\pi^+, K^+)\Lambda$ and $n(K^-, \pi^+)\Lambda$ or in the photo- and electroproduction reactions, e.g. $p(\gamma^*, K^+)\Lambda$ (see figure 2.1). However, the strangeness production, being far more general (reacher) process than the pion production extends our knowledge of the reaction mechanism to larger flavour space [7].

The pion induced process (π^+, K^+) is known as a strangeness creation (fig. 2.1 b), whereas in the process induced by antikaons (K^-, π^-) , the strangeness is transferred between the hadrons (fig. 2.1 a). The cross section of the latter process is the biggest one ($\approx mb$), but the luminosity is low and therefore the production role of this reaction is small. In the electromagnetic

process (γ^* , K^+), a pair of strange quarks has to be produced (fig. 2.1 c) which suppresses the cross section ($\approx nb$). However, the luminosity can be increased significantly using a high intensity electron beam (e.g. CEBAF in the Thomas Jefferson Laboratory, USA).

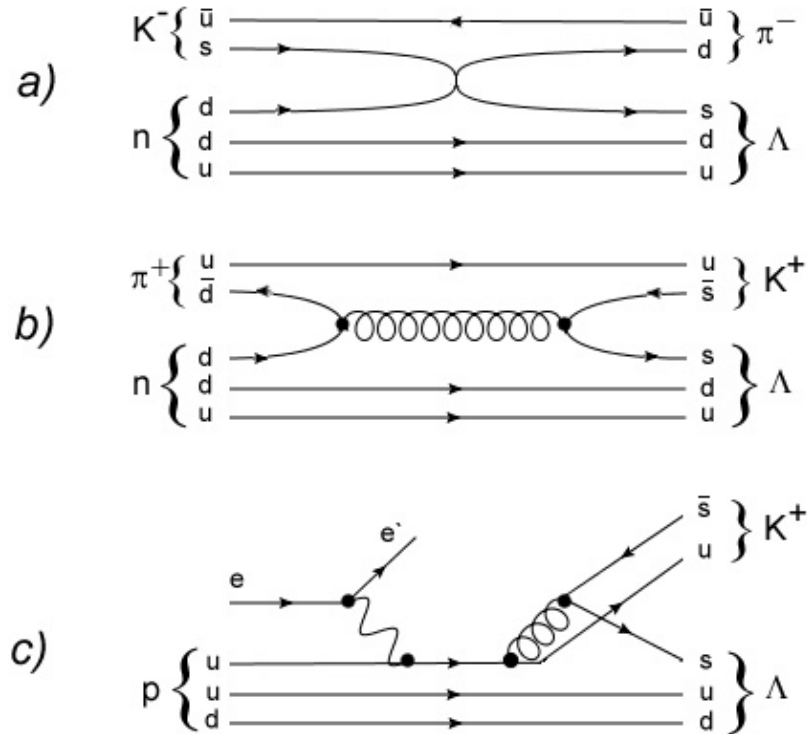


Figure 2.1: The particle production processes mentioned above in the text are shown. The figure *a* represents the process $n(K^-, \pi^-)\Lambda$ where the strangeness is transferred between the hadrons. The figure *b* represents the strangeness creation in the pion induced process $n(\pi^+, K^+)\Lambda$. Finally, the figure *c* shows the electromagnetic process $p(e, e' K^+)\Lambda$ where a pair of strange quarks is produced.

Although the largest count rates are obtained in the hadronic processes, use of an electromagnetic probe has a different advantage. Indeed, all electromagnetic ingredients in the reaction amplitude can be directly expressed in the context of the quantum electrodynamics (QED), the well-established theory of electromagnetic interactions [1,3].

2.3 What are the advantages of (γ^*, K) ?

A detailed study of electromagnetic production reactions

$$e + p \longrightarrow e' + \Lambda + K^+$$

$$e + p \longrightarrow e' + \Sigma^0 + K^+$$

$$e + p \longrightarrow e' + \Sigma^+ + K^0$$

$$e + n \longrightarrow e' + \Lambda + K^0$$

$$e + n \longrightarrow e' + \Sigma^0 + K^0$$

$$e + n \longrightarrow e' + \Sigma^- + K^+$$

is considerably more challenging than the pion production $p(\gamma, \pi^+)n$. One reason for that statement is that at present, high-duty electron and photon facilities like CEBAF, MAMI, ELSA, SPring-8, etc. provide data for electromagnetically induced reactions on the nucleon with unprecedented accuracy [7]. Moreover, gaining the information about the nucleon spectrum is far easier from the process (γ^*, K^+) than from the hadron induced reactions, because the electromagnetic part of the interaction is well-known and simpler to interpret. Theoretical approaches to electromagnetic strangeness production generally fall into two categories. The different approaches will be discussed later.

Associated strangeness production reactions are particularly interesting due to the creation of a strange quark-antiquark pair. In particular, the inclusion of a strange quark-antiquark pair in the reaction opens an additional degree of freedom, and it is believed that some of the missing resonances have a specific strong coupling into these “strange channels” [7].

On the other hand, the main difficulty in the kaon production, compared with the π and η production cases, is that the reaction mechanism here is not dominated by a small number of resonances, which then makes an analysis less transparent. This fact implies that we need to embody in the model contributions from a large number of resonances. According to the spin of the resonances, one needs one to five free parameters per resonance [9].

2.4 Historical Background

The beginning of both theoretical and experimental study of kaon photo- and electroproduction was given in the year 1957, when both Caltech and Cornell laboratories released the $p(\gamma, K^+)\Lambda$ cross-section data obtained at their electron synchrotrons. There were a plenty of data collected on the kaon photoproduction (Caltech, Cornell, etc. [3]) but only a few experiments were realized on the electroproduction (DESY, Cambridge [3]).

The modeling of kaon photoproduction processes started by the pioneering works of Kuo and Thom [6]. The few datapoints reported in these pioneering publications were of a limited accuracy, and only the kinematical region very close to threshold could be probed due to the limited electron energies available at that time.

Further experiments were performed in the 1970s and 1980s, not only in the USA but also at facilities in Bonn and Tokyo [3]. One had to wait until the end of nineties, when in the year 1998 the SAPHIR collaboration,

operating at the Bonn ELSA facility, released the first high precision data for all three reaction channels on the proton target

$$\gamma + p \longrightarrow K^+ + \Lambda, \quad (2.1)$$

$$\gamma + p \longrightarrow K^+ + \Sigma^0, \quad (2.2)$$

$$\gamma + p \longrightarrow K^0 + \Sigma^+, \quad (2.3)$$

over the photon laboratory energy range from threshold up to 2 GeV [3]. The reaction (2.1) is by far the most studied one, both experimentally and theoretically, although a large part of the existing data base suffers from inconsistencies within the reported accuracies. There are less investigations of the reaction (2.2). The third process has up to the mid-nineties received very little attention because of experimental difficulties in identifying the final state particles [5].

The SAPHIR data clearly triggered revived interest in the theoretical community in the search for missing resonances [11].

Over the past years, the database of the process (γ^*, K^+) has been substantially extended with a high precision data from the CLAS (2005, 2007 and 2010), SAPHIR (2003), LEPS (2003, 2006 and 2007) and GRAAL (2007) collaborations. In addition, the SAPHIR collaboration has also provided a new analysis of the $\gamma + p \rightarrow K^0 + \Sigma^+$ channel [3].

Chapter 3

Approaches to the Description of Particle Production Processes

Generally, the theoretical description of the electro- and photoproduction processes goes along two main paths. On the one hand, there are parton based models. It is the quark model which is at the basis of calculations of the reaction dynamics. The Regge theory, which is the high energy theory, also take the partonic constituents into account. The chiral perturbation theory, which is a low energy approximation of the QCD formalism, have to be remarked, too [4].

On the other hand, the problem can also be faced starting from solely hadronic degrees of freedom. In such an approach, the hadrons are treated as effective particles with specific properties. This kind of approach is the Isobar model, which is discussed in the next chapter.

From this dual approach, we hope to get a deeper level of understanding of the phase transition between the low and high energy description of the

subatomic matter [4].

3.1 χ PT, Quark Model, Regge Formalism, Regge-Plus-Resonance Approach

In the last few years, the chiral perturbation theory (χ PT) turned up as the powerful scheme to describe the low-energy meson-meson and meson-baryon dynamics. However, it is limited only to low energies (this means energy range from threshold up to approximately 100 MeV) and thus it can not describe the physics close to resonances [10]. Consequently, it is one of the possible approaches to the reaction (γ^* , K^+), though applicable only in the threshold region [13]. In order to simplify the approach, in the χ PT only the hadronic degrees of freedom are used (the approach would be far more complicated if the quark degrees of freedom played any role).

The quark model allows us to perform elementary approaches to study the reaction mechanism of $\gamma + p \rightarrow K^+ + \Lambda$. This model is in a closer connection with QCD than those based on the hadronic degrees of freedom. It needs a smaller number of parameters to describe the data [15]. In fact, it contains only a few coupling constants which are related together and there is no need to introduce the resonances, because they emerge naturally from the model as excited states of the system. The quark models therefore assume explicitly the extended structure of the hadrons which was found to be important for a reasonable description of the photoproduction data. In the quark model we usually restrict ourselves to the nonrelativistic description [13].

By definition, the quark model describes nucleon as a bound state of three constituent quarks. Although, the quark model predicted a plenty of resonances, some of them have not been proven experimentally yet. There are two possible explanations for this problem of “missing resonance”. The

first and more drastic one, that constituent quarks might not represent the proper degrees of freedom. Quark-diquark models, which contain fewer degrees of freedom, may be more convenient. On the other hand, the possibility that these resonances do exist, but manifest themselves in different reaction channels was indicated [3].

The Regge theory has a rich history which goes back to the late fifties and has proven to be an efficient approach for understanding a variety of high energy reactions involving hadronic and electromagnetic probes. It is an alternative approach to quantum mechanical potential scattering.

In its simplest form, the Regge model can be formulated as a modified version of the isobar approach. The main difference and the basic idea as well, is the property of Regge model, that each intermediate state in the Regge amplitude consists of several hadrons, rather than a single meson or baryon. The members of such a class of particles are characterized by a relation between their spin and mass squared. They are said to lie on a Regge trajectory [3,12].

The Regge model can constitute a direct link between the hadronic and partonic picture of certain processes.

The Regge amplitude is substantially simpler than the amplitude of an isobar model, because it does not contain resonances and consists only of background diagrams [14]. Therefore, the Regge model is a high-energy approach; it was developed mainly for the energy range beyond the resonance region $E_{\gamma}^{lab} > 4$ GeV and for small kaon angles [13,14]. On the other hand, the low-energy cross sections (in the resonance region) can not be reproduced in a pure background model. Nevertheless, this barrier can be overcome by adding to the Regge amplitude amount of Feynman diagrams which contain the intermediate nucleonic excitations, resonances. These resonant contributions are made to vanish sufficiently fast at high energies, where the pure

Regge model is valid. In that way, the Regge-plus-resonance model (the abbreviation we will use in the whole thesis is RPR) is developed [3].

The RPR approach has a plenty of benefits, we mention two of them. Firstly, a suitable high-energy behavior for the observables is automatically ensured. Secondly, the fact that the high-energy amplitude is given purely by its non-resonant (background) part allows us to determine the parameters of the background part from the high-energy data [3].

3.2 Coupled-Channel Approach

The final-state interaction is the general expression for meson-baryon rescattering processes among the hadrons in the final state which connects various channels of the process [13]. For instance, the reaction channels $\gamma + p \rightarrow K^+ + \Lambda$ and $\gamma + p \rightarrow \pi^+ + n$ are, due to the final-state interaction, coupled together. Therefore, we need to include both of them. This method is called the coupled-channel analysis and the models are unitary models (the \mathbb{S} matrix included is unitary). In other words, in the unitary models all possible final states of the electromagnetic-production part of the process are included. In principle, this would require information on channels, such as $K^+ + \Lambda \rightarrow K^+ + \Lambda$, for which no experimental information is available [11].

Accordingly, if we neglect the final-state interaction (this means restriction to only one-channel description), then the unitarity is broken.

To give an example, let us assume an s-channel graph with a nucleonic resonance. This resonance can decay in several ways (the probabilities and final products of the decay can be found in the Particle Data Booklet). As shown in figure 3.1, the probable way of the decay is $N^* \rightarrow K^+ + \Lambda$ (for the resonances $N(1650)$, $N(1710)$ and $N(1720)$ the probability is about 5-15

%). In fact, both K^+ and Λ interact strongly and therefore it comes to an rescattering process $K^+ + \Lambda \rightarrow K^+ + \Lambda$ described by the t-matrix in fig. 3.1 a. Another way of decay of the nucleonic resonance is $N^* \rightarrow \pi^+ + n$. Then the final-state interaction allows to couple both decay channels: $\pi^+ + n \rightarrow K^+ + \Lambda$. As can be seen from the figure, if we handle only the channel $\gamma + p \rightarrow K^+ + \Lambda$ (fig. 3.1 a) ignoring the second way of the decay we lose some flux in the final state.

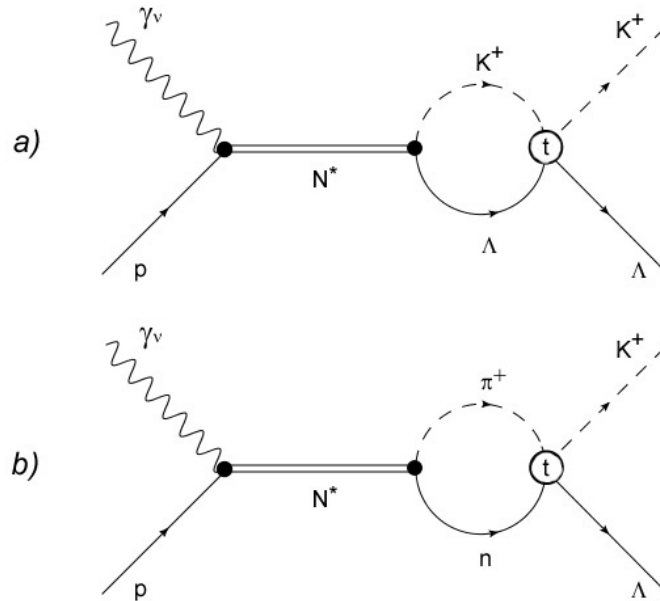


Figure 3.1: The s-channel graphs with a nucleonic resonance N^* are shown. The part *a* shows the nucleonic decay $N^* \rightarrow K^+ + \Lambda$ and the rescattering process $K^+ + \Lambda \rightarrow K^+ + \Lambda$, which gives the main contribution to the (γ^*, K^+) process. On the contrary, the figure *b* shows another way of decay of the nucleonic resonance $N^* \rightarrow \pi^+ + n$ which then through the final-state interaction gives the required $K^+ \Lambda$ final state: $\pi^+ + n \rightarrow K^+ + \Lambda$.

In principle, a complete coupled-channel analysis could handle the challenging problem of extracting the relevant physics form the meson scattering and meson production data. Apart form a unified description of a wide variety of reactions, a coupled-channel approach can incorporate the effect of

the final-state interactions into a description of the dynamics.

Obviously, the main advantage of the coupled-channel analysis is the larger amount of data which is at disposal. On the other hand, there is nothing we know about the amplitude of $K^+ + \Lambda \rightarrow K^+ + \Lambda$, which then have to be parametrized somehow [11]. Therefore, more parameters need to be introduced.

Chapter 4

Isobar Model

Since the early work of Thom [6] in the mid-sixties, great effort has been put into developing a model for the description of the $p(\gamma, K^+)\Lambda$ processes.

Firstly, let's introduce the main thoughts of the isobar model. The starting point for modeling the $p(\gamma, K^+)\Lambda$ processes is a description in terms of hadronic degrees of freedom. This means that in these models the reaction amplitude is derived from an effective hadronic Lagrangian using the Feynman diagrammatic technique in the tree-level approximation [3]. But even at the tree level, the description of this processes involves a substantial number of Feynman diagrams. The Feynman diagrams contribute into the background (or nonresonant) and the resonant part of the amplitude. The diagrams containing the intermediate nucleon excitations (or resonances) are referred to as the resonant diagrams, as they can produce peaks in the cross section (see fig. 4.1). The resonant diagrams reflect themselves as the s -channel terms and contain the most relevant physical information. Conversely, the diagrams with intermediate kaon and hyperon and their resonances, which cause no such behavior, are called background diagrams (see fig. 4.1) [3].

This kind of description (i.e. the tree-level effective-field approach) is

commonly referred to as the isobar model. It is the near-threshold and resonant kinematic region involving photon-laboratory energies $E_\gamma^{lab} = 0.91 - 2.5$ GeV, where the isobar model is of a particular interest [13].

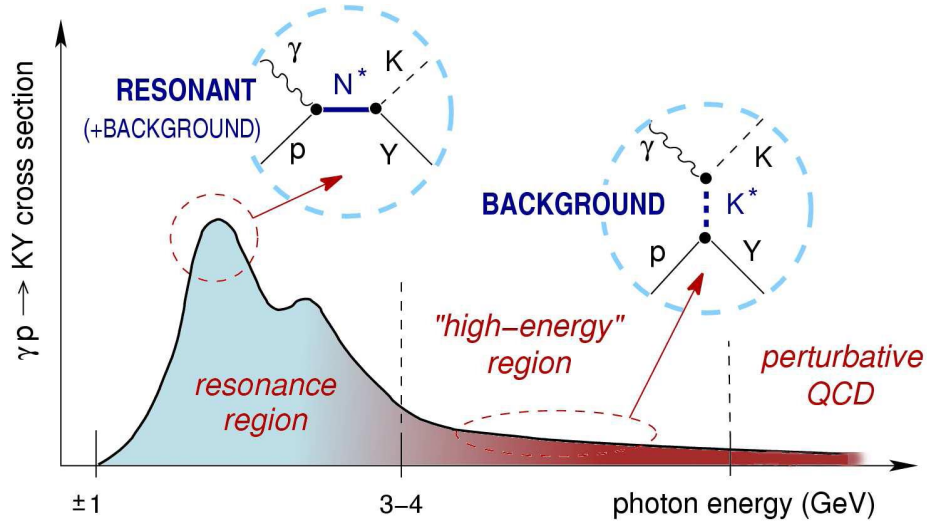


Figure 4.1: There is shown the schematic representation of the total KY (where $Y \equiv \Lambda, \Sigma^0, \Sigma^+$) photoproduction cross section as a function of the incoming photon energy in the lab frame E_γ^{lab} . The figure is from Ref. [3].

The effective-field approaches can, in principle, provide a direct connection between quark-model predictions for mesonic or baryonic properties and quantities accessible from experiments, such as the scattering cross sections.

Now it is the right time to clarify the term effective. Except at very high energies the current quarks and gluons do not represent the optimum building blocks in models of hadronic reactions. More convenient degrees of freedom are the constituent quarks surrounded by a cloud of gluons and quark-antiquark pairs forming mesons. As we can not fully describe properties of constituent quarks from a more fundamental field theory (QCD), they are referred to as effective degrees of freedom and are treated phenomenologically. Which effective building blocks to use depends on the energies and

momentum transfer involved in the process one needs to describe. In the kinematical region assumed here (the non-perturbative QCD region) it is natural to use hadrons in their entirety as effective degrees of freedom [3].

Despite the long history and the large amount of both experimental and theoretical efforts, a complete understanding of the $p(\gamma, K^+)\Lambda$ reaction mechanisms in this model remains troublesome. Firstly, there are many nucleon and hyperon resonances that contribute to the process, which results in a large number of versions of the isobar model [13]. Secondly, the Born terms in their own predict the $p(\gamma, K^+)\Lambda$ cross sections which are a few times the measured ones [12].

4.1 The Effective Lagrangian

The inter-particle interactions are modeled in terms of effective Lagrangians. In this approach, every intermediate particle in the reaction dynamics is treated as an effective field with its own characteristics such as mass, constants for coupling to electromagnetic and other hadronic fields and strong decay widths [3].

The effective-field theory determine the structure of propagators and the vertices which serve as input when calculating the different Feynman diagrams contributing to the reaction process.

Because the mathematical structure of these Lagrangians is not a priori known, their construction relies for the most part on symmetry arguments. In the effective-field theory, the various strong and electromagnetic coupling constants are not determined by the theory itself. They are treated as free parameters and can be determined either from the experiment by fitting the observable quantities to data or by relating to more fundamental models [3].

4.2 An Illustrative Calculation

In this section, we will deal with the electroproduction process and show how to calculate the invariant amplitudes or cross sections (for more detail see App. A).

Firstly, we write down the invariant amplitude of the process $e(p_e) + p(p_p) \rightarrow e'(p'_e) + \Lambda(p_\Lambda) + K^+(p_{K^+})$ in the one-photon-exchange approximation, which is as follows

$$iM_{fi} = \bar{u}_e(p'_e)(-ie\gamma^\mu)u_e(p_e) \left(\frac{-ig_{\mu\nu}}{q_\gamma^2} \right) \mathbb{J}^\nu(p_p, p_\Lambda, q_\gamma), \quad (4.1)$$

where $p_e = (E_e, \vec{p}_e)$ are the fourvectors and $q_\gamma = p'_e - p_e$, $q_\gamma^2 < 0$ is the momentum of a virtual photon; u is the Dirac spinor; γ^μ is the Dirac matrix; $g_{\mu\nu}$ the metric tensor; and \mathbb{J}^ν is the matrix element of the hadron flux, which describes the photoproduction of a kaon on proton induced by the virtual photon.

In the equation (4.1), the contribution of the electron part of the diagram is given explicitly and therefore one needs only to calculate the matrix element \mathbb{J}^ν . For the description of this, the effective hadronic Lagrangian in the tree-level approximation is used. Schematically, the single contributions (the reducible part) are shown in the figure 4.2.

For illustration, we evaluate the first contribution of the scheme on the figure (that is the proton exchange, s -channel). The matrix element then reads

$$\mathbb{J}_{(1)}^\nu = \bar{u}_\Lambda(p_\Lambda)\gamma_5 g_{pK\Lambda} \frac{P + m_p}{s - m_p^2} \left[-ie\gamma_\nu + \mu_p \frac{e}{2m_p} \sigma_{\nu\mu} q_\gamma^\mu \right] u_p(p_p), \quad (4.2)$$

where $g_{pK\Lambda}$ is the coupling constant of the vertex with kaon and Λ hyperon; γ_5 is the Dirac matrix, $P = p_p + q_\gamma$, $s = P^2$, $\sigma_{\nu\mu} = \frac{i}{2} [\gamma_\nu, \gamma_\mu]$. The

first term in the bracket is for the vector coupling and the second term for the tensor coupling caused by the anomalous magnetic moment of the proton (μ_p).

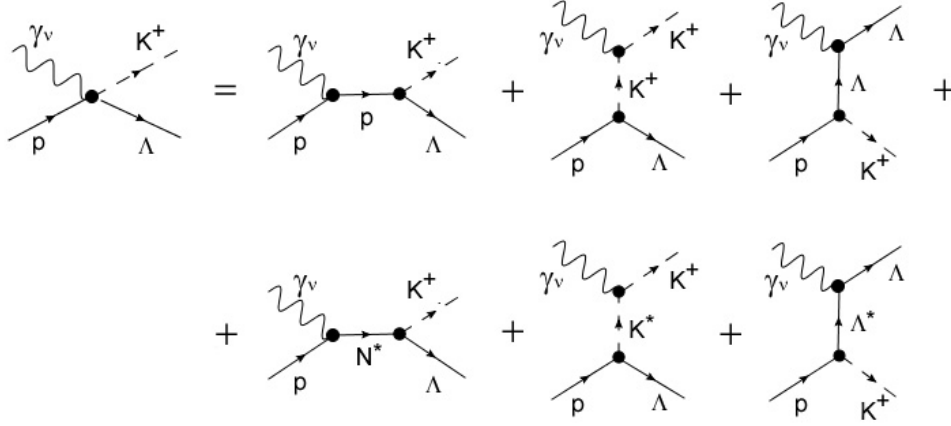


Figure 4.2: There are shown different elements of the lowest-order $p(\gamma^*, K^+)\Lambda$ amplitude. The upper line collects the Born terms, which have a ground-state hadron in the intermediate state. Depending on whether the exchanged particle is a proton, a kaon, or a hyperon, one distinguishes between s-, t- and u-channel contributions, respectively. The lower line shows the non-Born terms [3].

For further calculations it is needed to express the scalar amplitudes \mathcal{A}_j (see App. A) from equation (4.2). By a suitable manipulation of the terms in that equation, one obtains

$$\mathbb{J}_{(1)}^\nu = -i\bar{u}_\Lambda(p_\Lambda)\gamma_5 \left[\mathcal{A}_1^{(1)}M_1^\nu + \mathcal{A}_2^{(1)}M_2^\nu + \mathcal{A}_4^{(1)}M_4^\nu - \mathcal{A}_6^{(1)}M_6^\nu + eg_{pK\Lambda}\frac{q_\gamma^\nu}{q^2} \right] u_p(p_p),$$

where expressions for $\mathcal{A}_j^{(1)}$ are given in App. A.

The last term in the bracket, which violates the gauge invariance, vanishes in the full tree-level approximation, because the counter term emerges from the second contribution in figure 4.2 - the kaon exchange.

4.3 Properties of the Model

4.3.1 Resonances

The meson production processes are suitable to probe the properties of the resonances. In quark model calculations, there are far more excited states than observed in the experiments, which is known as the “missing resonance” phenomenon.

There are more than twenty resonances as likely candidates to participate in the $p(\gamma, K^+)\Lambda$ reaction. A number of those resonances is only poorly characterized. It is believed that they all have large widths of hundreds of MeV, resulting in a broad energy smudging of every state [4].

Moreover, several calculations have shown that the data gathered from experiments can not be reproduced without including some particular resonances. Thereby, the calculations provide indirect support for the existence of these excited states. Therefore, special attention is paid to the problem of “missing resonances” and to searching for their signals [11]. By determining the various resonance contributions, one can extract values for the coupling constants [4].

Furthermore, as was mentioned in the beginning of this chapter, the cross sections when given only by the Born terms are a few times the measured ones. However, it turns out that hyperon resonances and hadronic form factors can provide a natural mechanism to produce theoretical cross sections of the right order of magnitude [12].

4.3.2 Coupling Constants

An effective Lagrangian approach for the $p(\gamma, K^+)\Lambda$ process involves the introduction of a set of coupling constants. Being parameters in an effective theory, these coupling constants can be, in principle, calculated on the basis

of QCD-inspired constituent-quark models for the hadrons. Consequently, the effective field theories allow to test theoretical predictions for coupling constants against photoproduction data.

Assuming the SU(3) flavour symmetry, the coupling constants $g_{K\Lambda p}$ and $g_{K\Sigma^0 p}$, which serve as input parameters when computing the Born contributions, are fixed by the well-known $g_{\pi NN}$ coupling. One of the striking observations when dealing with the $p(\gamma, K^+)\Lambda$ process in terms of hadronic degrees of freedom, is that the Born terms on their own give rise to cross sections which largely overshoot the data, strictly speaking this statement is valid only in the case, when the SU(3) limits for the coupling constants $g_{K\Lambda p}$ and $g_{K\Sigma n}$ are considered [13].

4.3.3 Hadronic and Electromagnetic Form Factors

Due to the final structure of the hadrons, the vertices can not be treated as interactions of point-like particles. To account for the finite extension of the hadrons, it is a common procedure to introduce a phenomenological form factor at each strong or electromagnetic (for the electroproduction) vertex. Therefore, we set up for example a dipole form factor to modify each hadronic vertex. The widely used form factor is of the type

$$F_x(\Lambda) = \frac{\Lambda^4}{\Lambda^4 + (x - M_x^2)^2},$$

where $x \equiv s, t, u$; Λ is the cutoff value and sets the short-distance scale of the effective theory and x represents the off-mass-shell momentum squared at the vertex.

It is well-known that introducing the hadronic form factors violates the gauge invariance at the level of the Born diagrams. Additional contact term is then required to restore this fundamental symmetry [12].

In the electroproduction, one needs to introduce the electromagnetic form factor in the photon vertex [8], see fig. 4.3.

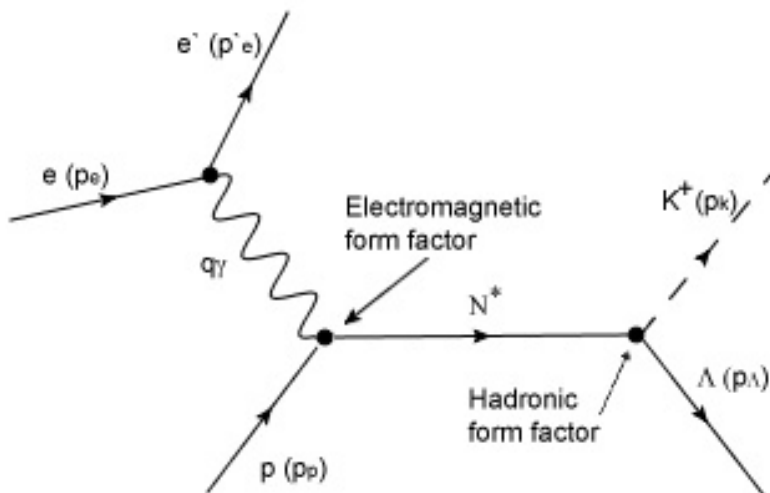


Figure 4.3: Electromagnetic and hadronic form factors

4.3.4 Amplitudes and Observables

Because of historical and practical reasons (the nuclear calculations) the two-component spinor representation of the amplitude is often used. In this form the full amplitude can be expressed in terms of six Chew-Goldberger-Low-Nambu (CGLN) amplitudes \mathcal{F}_j

$$\begin{aligned}
 \mathcal{F} = & \sigma \cdot \hat{\varepsilon} \mathcal{F}_1 + i(\sigma \cdot \hat{p}_K)(\sigma \times \hat{p}_\gamma \cdot \hat{\varepsilon}) \mathcal{F}_2 \\
 & + (\sigma \cdot \hat{p}_\gamma)(\hat{p}_K \cdot \hat{\varepsilon}) \mathcal{F}_3 + (\sigma \cdot \hat{p}_K)(\hat{p}_K \cdot \hat{\varepsilon}) \mathcal{F}_4 \\
 & + (\sigma \cdot \hat{p}_\gamma)(\hat{p}_\gamma \cdot \hat{\varepsilon}) \mathcal{F}_5 + (\sigma \cdot \hat{p}_K)(\hat{p}_\gamma \cdot \hat{\varepsilon}) \mathcal{F}_6,
 \end{aligned} \tag{4.3}$$

where we used $\hat{a} \equiv \frac{\vec{a}}{|\vec{a}|}$. There are many prescriptions used in the literature, the one we use stems from Ref. [5]. Relations of the CGLN amplitudes to the scalar amplitudes \mathcal{A}_j are given in App. A.1.

The electroproduction cross sections are then obtained as

$$\begin{aligned} \frac{d\sigma}{d\Omega} = & d\sigma_U + \varepsilon_L d\sigma_L + \varepsilon d\sigma_P \sin^2(\theta) \cos(2\phi) \\ & + \sqrt{2\varepsilon_L(1 + \varepsilon)} d\sigma_I \sin(\theta) \cos(\phi). \end{aligned} \quad (4.4)$$

In this equation, θ is the angle between the outgoing kaon and the virtual photon, and ϕ is the azimuthal angle between the kaon production plane and the electron scattering plane (see fig. 4.4). Parameters ε and ε_L are the transverse and longitudinal polarization parameters, respectively. Moreover, $d\sigma_U$ is the cross section for an unpolarized incident photon beam, and the term containing $d\sigma_P$ is the asymmetry contribution of a transversally polarized beam. The cross section of a longitudinally polarized virtual photon is given by $d\sigma_L$, while $d\sigma_I$ contains the interference effects between the longitudinal and transverse components of photon [5].

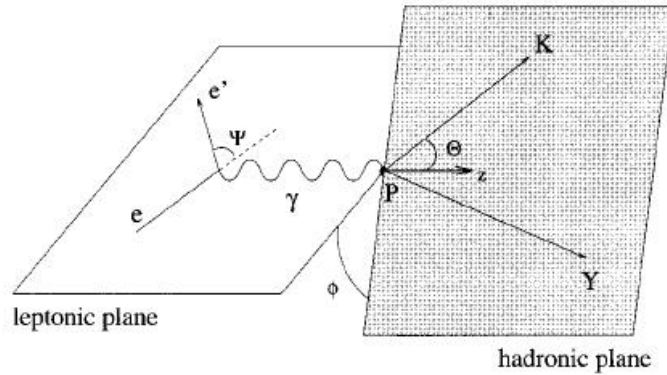


Figure 4.4: Leptonic and hadronic planes for kaon electroproduction. Figure is from Ref. [5].

Chapter 5

Demonstrative Calculations and Graphs

In this chapter, the graphs of the cross section depending either on the kaon angle in the center of mass frame $\theta_K^{c.m.}$ or on the total center-of-mass energy W are shown. The data were collected from the plenty of experiments (see the legend in the figures 5.1 and 5.2), but only the Kaon-MAID model was used to describe them. It would be useful to introduce main thoughts of this model.

Besides the extended Born diagrams (exchanges of proton, K^+ , Λ and Σ^0 particles), the Kaon-MAID model also includes exchanges of resonances in s- and t-channels:

- in the t-channel - vector $K^*(890)$ and axial vector $K_1(1270)$
- in the s-channel - $S_{11}(1650)$, $P_{11}(1710)$, $P_{13}(1720)$ and a “missing resonance” $D_{13}(1895)$

On the contrary, the model does not include any exchange of hyperon resonances in the u-channel.

In the strong vertices, hadronic form factors are assumed in the line of Haberzettl [19], which preserve the gauge invariance of the model. Values of the main coupling constants, $g_{K\Lambda N}$ and $g_{KN\Sigma}$, fulfil the flavour SU(3) symmetry.

The crossing symmetry, which relates the photoproduction channel with the process of radiative capture (the crossing symmetry gives $\gamma p \rightarrow K^+\Lambda \leftrightarrow K^-p \rightarrow \Lambda\gamma$), is not taken into account in this model.

Parameters of the model (coupling constants and cut-offs) were fitted to the old SAPHIR data from the year 1998 [19].

On the figure 5.1, there is shown the dependence of the cross section on the kaon angle in the center of mass frame $\theta_K^{c.m.}$. The data were collected at fixed photon-laboratory energy at about 1.32 GeV (the energy vary from one data set to another at most by 0.01 GeV). Remarkable but well-known attribute of the experimental data is their inconsistency in the small kaon angles. This gives the room for further improvement in the experiments.

On the figure 5.2, the cross section depending on the total c. m. energy W is shown. The data were obtained from CLAS collaboration in the year 2005 with fixed kaon angle at about 37° ($\cos \theta_K^{c.m.} = 0.8$).

The continuous line represents the Kaon-MAID model. As can be seen from the figure, the model is in good agreement with the experimental data only up to the energy of $W = 2.2$ GeV. This is caused by the fact, that the Kaon-MAID model was fitted with the old data, which were measured only within the energies $W = 1.6 - 2.2$ GeV.

The dashed curve shows the model without the $D_{13}(1895)$ resonance. It can be seen, that this resonance is important for the description of data around the energy of $W = 1.9$ GeV.

The dotted curve illustrates how the model describes the data when the $P_{13}(1720)$ resonance is omitted. According to the fig. 5.2, this resonance is

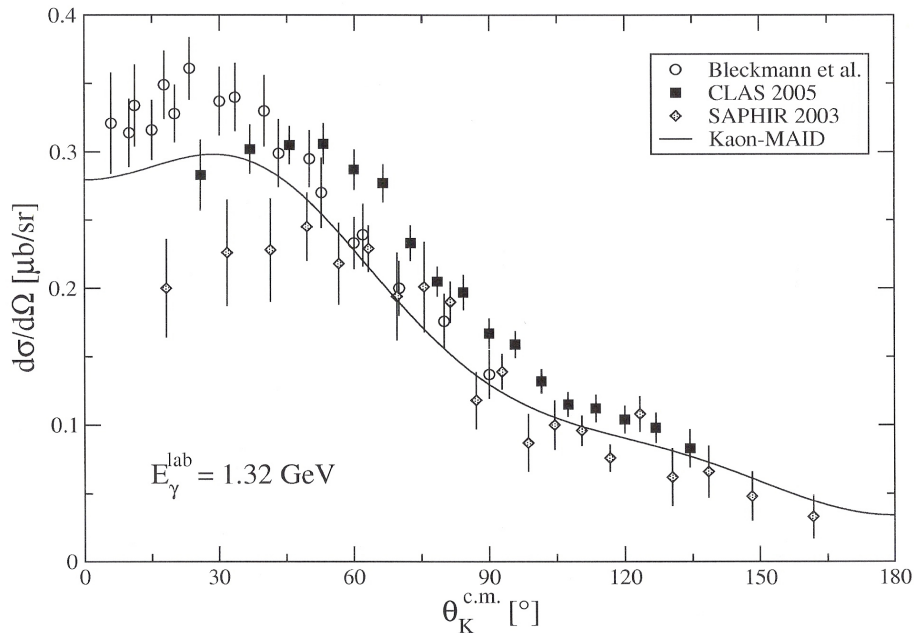


Figure 5.1: The cross section in dependence on the kaon angle in the center of mass frame is shown. The photon-laboratory energy is fixed approximately at 1.32 GeV. It is well-known, that in the small angles, the data suffer from noticeable inconsistency. This brings the room for further experiments and better analysis. The data represented in the figure by circles originates from Ref. [16], the data represented by squares from Ref. [17] and the data represented by diamonds from Ref. [18]

needed for a good agreement with the data in the energy range $W = 1.6 - 2.0 \text{ GeV}$, although one can expect a drop only in the region around $W = 1.7 \text{ GeV}$. This could be caused by the coupling (interference) with another resonances. What else could play a role is, that the resonances differ by the relative ratio of their coupling constants for vector and tensor part.

The dash-dotted curve shows the model without all nucleonic resonances as a smooth function of energy. The main part for the grow up in the energy range $W > 2.2 \text{ GeV}$ is made by the vector kaon resonance $K^*(890)$.

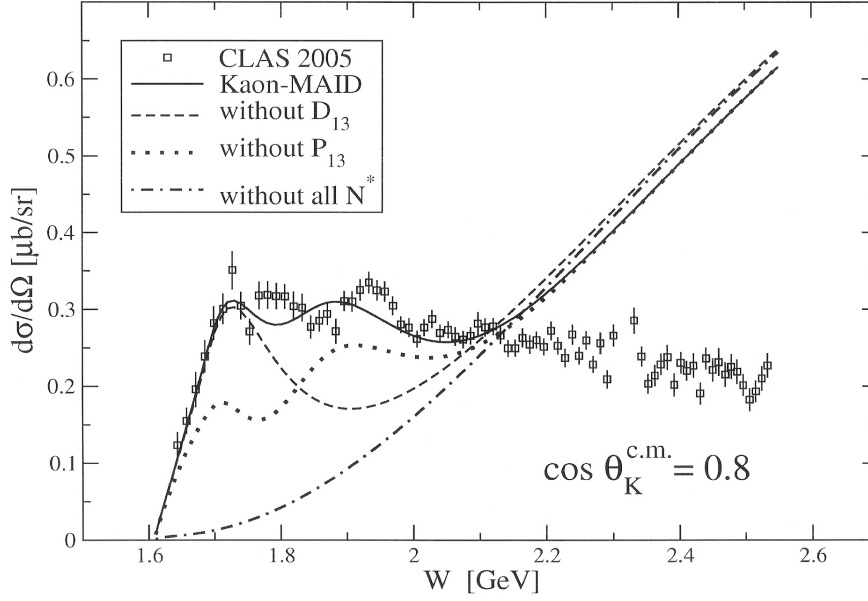


Figure 5.2: The cross section in dependence on the total c. m. energy is shown. The experimental data originate from CLAS 2005 [17]. The continuous line represents the Kaon-MAID model, which is in a good agreement with the data in the energy range $W = 1.6\text{--}2.2$ GeV. The dashed, dotted and dash-dotted lines illustrates the description of the data without D_{13} resonance, P_{13} resonance and all nucleonic resonances, respectively.

For the calculation the program EMKHYP and also the web pages of the Kaon-MAID model [19] were used.

Chapter 6

Conclusion

This thesis showed the basic properties of the photo- and electroproduction processes, the rich history of their investigating and reasons, why these processes are important for modern-day physics .

The theoretical approaches to the description of these processes were sketched, too. But a special room in this thesis was reserved for the tree-level effective-field approach, the Isobar model, which is of particular interest.

Thanks to the importance of the photo- and electroproduction processes (we expect to gain a deeper insight into the hadron structure), the experimental community is interested in the search for missing resonances, which brings a flood of initiatives for the theoretical community. Many approaches to describe the photo- and electroproduction processes have been developed, but there is still room for questions and for the further analysis, as was shown in the fifth chapter (for example the problem with the unlike cross sections for different data sets).

Because of many of these unanswered questions, this topic could be very interesting for researching in the next years.

Appendix A

The Hadron Current

The hadron current for the virtual-photon production process

$$\gamma^*(q_\gamma) + p(p_p) \rightarrow K^+(p_K) + \Lambda(p_\Lambda)$$

is convenient to write down in a general form given by gauge and Lorentz symmetries as

$$\mathbb{J}^\nu(p_p, p_\Lambda, q_\gamma) = \sum_{j=1}^6 \mathcal{A}_j(s, t, q_\gamma^2) \bar{u}_\Lambda(p_\Lambda) \gamma_5 M_j^\nu u_p(p_p),$$

where M_j^ν are the gauge invariant operators, for which $M_j^\nu q_{\gamma\nu} = 0$, and \mathcal{A}_j are scalar amplitudes, which in the isobar model result from contributions of particular Feynman diagrams. For the operators M_j^ν , there are many prescriptions used in the literature. The one we use in this thesis is

$$\begin{aligned} M_1^\nu &= \frac{1}{2} (\not{q}_\gamma \gamma^\nu - \gamma^\nu \not{q}_\gamma), & M_2^\nu &= p_p^\nu - q_\gamma p_p \frac{q_\gamma^\nu}{q_\gamma^2}, \\ M_3^\nu &= p_\Lambda^\nu - q_\gamma p_\Lambda \frac{q_\gamma^\nu}{q_\gamma^2}, & M_4^\nu &= \gamma^\nu (q_\gamma p_p) - \not{q}_\gamma p_p^\nu, \\ M_5^\nu &= \gamma^\nu (q_\gamma p_\Lambda) - \not{q}_\gamma p_\Lambda^\nu, & M_6^\nu &= \not{q}_\gamma q_\gamma^\nu - \gamma^\nu q_\gamma^2. \end{aligned}$$

In section 4.2, the scalar amplitudes $\mathcal{A}_j^{(1)}$ for the proton exchange in the s-channel reads

$$\begin{aligned}\mathcal{A}_1^{(1)} &= -\mathbf{i}e \frac{g_{pK\Lambda}}{s-m_p^2} (1 + \mu_p), & \mathcal{A}_2^{(1)} &= -2\mathbf{i}e \frac{g_{pK\Lambda}}{s-m_p^2}, \\ \mathcal{A}_4^{(1)} &= -\mathbf{i}e \frac{g_{pK\Lambda}}{s-m_p^2} \frac{\mu_p}{m_p}, & \mathcal{A}_6^{(1)} &= -\frac{1}{2}\mathcal{A}_4^{(1)}.\end{aligned}$$

The amplitudes in the t-channel (the K^+ exchange) $\mathcal{A}_j^{(2)}$ reads

$$\mathcal{A}_2^{(2)} = 2e \frac{g_{K\Lambda p}}{t - m_k^2},$$

$$\mathcal{A}_3^{(2)} = -\mathcal{A}_2^{(2)}$$

A.1 CGLN Amplitudes

The relations between the CGLN amplitudes (in Eq. 4.3) and the scalar amplitudes \mathcal{A}_j are (the prescriptions are used from Ref. [5])

$$\mathcal{F}_1 = (\sqrt{s} - M_p)\mathcal{A}_1 - p_\gamma \cdot p_p \mathcal{A}_3 - p_\gamma \cdot p_\Lambda \mathcal{A}_4 - p_\gamma^2 \mathcal{A}_5,$$

$$\mathcal{F}_2 = \frac{|p_\gamma| \cdot |p_K|}{(E_p + M_p)(E_\Lambda + M_\Lambda)} [(\sqrt{s} - M_p)\mathcal{A}_1 - p_\gamma \cdot p_p \mathcal{A}_3 - p_\gamma \cdot p_\Lambda \mathcal{A}_4 - p_\gamma^2 \mathcal{A}_5],$$

$$\mathcal{F}_3 = \frac{|p_\gamma| \cdot |p_K|}{(E_p + M_p)} [-2p_\gamma \cdot p_p \mathcal{A}_2 + (\sqrt{s} + M_p)\mathcal{A}_4 + p_\gamma^2 \mathcal{A}_6],$$

$$\mathcal{F}_4 = \frac{|p_K|^2}{(E_\Lambda + M_\Lambda)} [2p_\gamma \cdot p_p \mathcal{A}_2 (\sqrt{s} - M_p)\mathcal{A}_4 - p_\gamma^2 \mathcal{A}_6],$$

$$\mathcal{F}_5 = \frac{|p_\gamma|^2}{(E_p + M_p)} [-\mathcal{A}_1 + 2p_\gamma \cdot p_\Lambda \mathcal{A}_2 + (\sqrt{s} + M_p)(\mathcal{A}_3 - \mathcal{A}_5) + p_\gamma \cdot p_\Lambda \mathcal{A}_6]$$

$$\mathcal{F}_6 = \frac{|p_\gamma| |p_K|}{(E_\Lambda + M_\Lambda)} [-2p_\gamma \cdot p_\Lambda \mathcal{A}_2 + (\sqrt{s} - M_p) \mathcal{A}_3 - p_\gamma \cdot p_\Lambda \mathcal{A}_6 - \frac{1}{E_p + M_p} (p_{\gamma 0} \mathcal{A}_1 + p_\gamma \cdot p_p \mathcal{A}_3 + p_\gamma \cdot p_\Lambda \mathcal{A}_4 + p_{\gamma 0} (\sqrt{s} + M_p) \mathcal{A}_5)],$$

Appendix B

Feynman diagrams

The formalism of Feynman diagrams is a calculation scheme introduced by Richard P. Feynman to represent the mechanisms of elementary-particle interactions. The Feynman-diagram technique is very important in the Quantum Electrodynamics (QED) for calculations of the cross sections and transition rates because the coupling constant α in the perturbation expansion is very small, $\alpha = 1/137$.

As we mentioned above, the Feynman diagrams are connected with the perturbation theory. The basic building block of the Feynman diagram is a vertex. Any physical process in QED involving the interaction of electrons, positrons, photons, etc. can be represented and the first step is to find a diagram with the least possible number of vertices. This simplest combination of vertices which give the required process is called a leading-order diagram (it is important to know that there may be more than one such diagram). The leading-order diagrams correspond to the lowest order of a perturbation calculation and have the biggest contribution to the total amplitude of the process.

In addition to the leading-order diagrams there are higher-order diagrams, each of which will contribute to the total amplitude. However, these con-

tributions are in magnitude at least α -times smaller than the leading order. It is the smallness of α which makes all but the next-to-leading-order contributions negligible. Since the higher-order diagrams can only be drawn by adding internal lines, they must always involve two more vertices for each step in increasing order.

In an effective field theory (e.g. the Quantum Hadrodynamics), the coupling constants need not to be small enough to justify the perturbation expansion and, therefore, one assumes only the lowest order(s) of the expansion, e.g. the tree level.

For the construction of the Feynman diagrams, only the topological structure is important. As long as the ordering of the vertices along the fermion lines is kept, the graphs can be arbitrarily deformed without changing their meaning.

B.1 The Rules for the Construction and Interpretation of Feynman Diagrams

There is a list of rules which needs to be obeyed when constructing Feynman diagrams. The first two rules are universal - these are the conservation laws. But there are six other rules that apply in the diagrams, too.

1. Energy and momentum are conserved at a vertex.
2. Electric charge is conserved at a vertex.
3. Solid straight lines with arrow that point in the direction of increasing time are used to represent fermions propagating forward in time. Arrow heads pointing in the reverse direction represent antifermions propagating forward in time.
4. Broken, wavy, or curly lines are used to represent bosons.

5. Lines having one end at the boundary of the diagram represent free (that means real) particles approaching or leaving a reaction.
6. Lines that join two vertices (internal lines) normally represent virtual particles.
7. The time ordering of the vertices connected by an internal line is not determined, so that two diagrams having an internal line apparently oriented differently with respect to time, but otherwise the same, are not different diagrams.
8. Every particle at the boundary should be labelled with a momentum. If this is done two diagrams which might otherwise appear to be the same become different diagrams.

All information about the Feynman diagrams stems from Ref. [1] and [2].

Bibliography

- [1] W. Greiner, J. Reinhardt, *Quantum Electrodynamics*, Springer-Verlag, Berlin, 2003
- [2] W.S.C. Williams, *Nuclear and Particle Physics*, Oxford University Press Inc., New York, 1991
- [3] Corthals T., *Regge-plus-resonance Approach to Kaon Production from the Proton*, PhD Thesis, Gent University 2006-2007
- [4] Janssen S., *Strangeness Production on the Nucleon*, PhD Thesis, Gent University 2001-2002
- [5] J.C. David, C. Fayard, G. H. Lamot and B. Saghai, Phys. Rev. C 53, 2613 (1996)
- [6] H. Thom, Phys. Rev. 151, 1322 (1966)
- [7] S. Janssen, J. Ryckebusch, D. Debruyne, T. Van Cauteren, Phys. Rev. C 65, 015201 (2001)
- [8] B. Saghai, In Proc. *Electrotoproduction of Strangeness on Nucleons and Nuclei*, edited by K. Maeda, H. Tamura, S. H. Nakamura, O. Hashimoto (World Scientific Publishing Co. Pte. Ltd., Singapore, 2004), page 54

- [9] A. Ramos *et al.*, In Proc. *Electrophotoproduction of Strangeness on Nucleons and Nuclei*, edited by K. Maeda, H. Tamura, S. H. Nakamura, O. Hashimoto (World Scientific Publishing Co. Pte. Ltd., Singapore, 2004), page 75
- [10] T. K. Choi *et al.*, In Proc. *Electrophotoproduction of Strangeness on Nucleons and Nuclei*, edited by K. Maeda, H. Tamura, S. H. Nakamura, O. Hashimoto (World Scientific Publishing Co. Pte. Ltd., Singapore, 2004), page 90
- [11] C. Bennhold *et al.*, arXiv:nucl-th/9901066v1 (1999)
- [12] S. Janssen, J. Ryckebusch, D. Debruyne, T. Van Cauteren, Phys. Rev. C 66, 035202 (2002)
- [13] P. Bydzovsky *et al.*, arXiv:nucl-th/0305039v1 (2003)
- [14] M. Guidal *et al.*, Phys. Rev. C 61, 025204 (2000)
- [15] M. K. Cheoun *et al.*, arXiv:nucl-th/9912011v1 (1999)
- [16] A. Bleckmann *et al.*, Z. Phys. 239, 1 (1970)
- [17] R. Bradford *et al.*, Phys. Rev. C73, 035202 (2006)
- [18] K. H. Glander *et al.*, Eur. Phys. J. A19, 251 (2004)
- [19] <http://wwwkph.kph.uni-mainz.de/MAID//kaon/> (1.7.2010)